Int. J. Heat Mass Transfer. Vol. 32, No. 4, pp. 665–677, 1989
Printed in Great Britain

0017–9310/89 $3.00 + 0.00

Analysis of natural convection about a vertical plate embedded in a porous medium

S. J. KIM and K. VAFAI
Department of Mechanical Engineering, Ohio State University, Columbus, OH 43210, U.S.A.

(*Received* 2 *May* 1988 *and in final form* 25 *August* 1988)

Abstract—Buoyancy-driven fluid flow and heat transfer about a vertical flat plate embedded in a porous medium are analyzed in depth for two general cases. These are the constant wall temperature case and the constant wall heat flux case. By an order of magnitude analysis it is shown that there are two governing dimensionless parameters which are related to the thermal and viscous effects. These are $Ra_L^{-1/2}$ and $Da_L^{1/2}$ for the constant wall temperature case and $Ra_L^{*-1/3}$ and $Da_L^{1/2}$ for the constant wall heat flux case. For each case, two important categories are considered. For the constant wall temperature case these categories are shown to be physically related to either $Da_L^{1/2} \ll Ra_L^{-1/2}$ ($Da_L^{1/2} \ll Ra_L^{*-1/3}$ for the constant wall heat flux) or $Da_L^{1/2} \gg Ra_L^{-1/2}$ ($Da_L^{1/2} \gg Ra_L^{*-1/3}$ for the constant wall heat flux). The governing equations are solved analytically using the method of matched asymptotic expansions along with the modified Oseen method. The numerical solution of the governing equations based on the similarity transformations is also obtained. It is found that the rate of heat transfer depends on the modified Rayleigh number for $Da_L^{1/2} \ll Ra_L^{-1/2}$ (or $Da_L^{1/2} \ll Ra_L^{*-1/3}$) while the Nusselt number depends on the product of the Rayleigh number and the porosity for $Da_L^{1/2} \gg Ra_L^{-1/2}$ (or $Da_L^{1/2} \gg Ra_L^{*-1/3}$). The heat transfer characteristics for the latter are shown to be independent of the permeability of the porous medium and approaching those of the regular fluid with a high Prandtl number. A complete physical description of the problem is presented throughout the analysis.

1. INTRODUCTION

THE MAJORITY of existing studies on convective heat transfer in porous media are based on the Darcy flow model. Darcy's law, however, is found to be inadequate for the formulation of fluid flow and heat transfer problems in porous media when there is a solid boundary and the Reynolds number based on the pore size is greater than unity. Therefore, it is necessary to incorporate the boundary and inertia terms into the momentum equation. These effects have been studied for forced convection [1–5] as well as for natural convection [6–9] in porous media.

The problem of natural convection about a heated impermeable surface embedded in fluid-saturated porous media was studied by Cheng and Minkowycz [10]. They obtained similarity solutions which were based on Darcy's law and boundary layer approximations. To extend the range of applicability of the boundary layer analysis to relatively lower modified Rayleigh numbers, Cheng and Hsu [11], and Joshi and Gebhart [12] examined higher order effects such as the entrainment from the edge of the boundary layer, the axial heat conduction, and the normal pressure gradient using the method of matched asymptotic expansions. A number of recent studies have considered the various non-Darcian effects on the same problem. Bejan and Poulikakos [7], and Plumb and Huenefeld [13] used Forschheimer's equation to account for inertia effects and obtained similarity solutions based on boundary layer approximations. Hsu and Cheng [8] and Evans and Plumb [14] studied the boundary effect on heat transfer and fluid flow based on Brinkman's equation. Hong *et al.* [9] included both the boundary and inertia effects as well as the convective term in the momentum equation. Also Kaviany and Mittal [15] studied natural convection from a vertical plate experimentally and reported Karman–Pohlhausen solutions for a high permeability porous medium. These investigators have shown that both the boundary and inertia effects decrease the heat transfer rate.

In this paper natural convection about a vertical flat plate in a fluid-saturated porous medium is considered based on the Brinkman-extended Darcy flow model. It should be noted that for this problem the power-law wall temperature variation no longer represents the case of the constant wall heat flux when either the higher order effects or the boundary effects are taken into account as pointed out in refs. [12, 16], respectively. Hence the case of the constant temperature and the case of constant heat flux are treated separately. Also it was shown in ref. [8] that there are two governing dimensionless parameters associated with this problem. These are ε_T and ε_V where $\varepsilon_T = Ra_L^{-1/2}$ and $\varepsilon_V = Da_L^{1/2}$ with Ra_L and Da_L as the modified Rayleigh number and the Darcy number, respectively. The thickness of the viscous boundary layer is of the order of ε_V and that of the thermal boundary layer is of the order of ε_T. Hence, depending on the thickness ratio of the viscous boundary layer to that of the thermal boundary layer there exists two categories. One is when $\varepsilon_T \gg \varepsilon_V$ and the other is when $\varepsilon_V \gg \varepsilon_T$. The former category was numerically studied in ref. [8], while the

NOMENCLATURE

Da_L	Darcy number based on L, $(1/L^2)(K/\delta)$
Da_x	local Darcy number, $(1/x^2)(K/\delta)$
g	gravitational acceleration
K	permeability of the porous medium
k_e	effective thermal conductivity of the saturated porous medium
L	reference dimensional length
Nu_x	local Nusselt number
p	pressure
Ra_L	modified Rayleigh number based on L, $Kg\beta L(T_w-T_\infty)/\nu_f\alpha_e$
Ra_L^*	modified Rayleigh number based on heat flux, $Kg\beta L^2q/k_e\nu_f\alpha_e$
Ra_x	local modified Rayleigh number, $Kg\beta x(T_w-T_\infty)/\nu_f\alpha_e$
Ra_x^*	local modified Rayleigh number based on heat flux, $Kg\beta x^2q/k_e\nu_f\alpha_e$
T	dimensional temperature
u	dimensionless velocity in the x-direction
v	dimensionless velocity in the y-direction
x	dimensional coordinate along the plate
y	dimensional coordinate perpendicular to the plate
Y	dimensionless coordinate in the outer layer, y
$\hat{Y}$	dimensionless coordinate in the inner layer, y.

Greek symbols

α_e	effective thermal diffusivity
β	thermal expansion coefficient of fluid
Γ_T	perturbation parameter for Case TI
Γ_H	perturbation parameter for Case HI
δ	porosity of the porous medium
Δ_T	perturbation parameter for Case TII
Δ_H	perturbation parameter for Case HII
$\eta_{1,2}$	similarity variable for Cases TI, TII
$\zeta_{1,2}$	similarity variable for Cases HI, HII
θ	dimensionless temperature
Θ	dimensionless temperature in the outer layer
$\hat{\Theta}$	dimensionless temperature in the inner layer
μ_f	fluid viscosity
ν_f	kinematic viscosity
ψ	dimensionless stream function
Ψ	dimensionless stream function in the outer layer
$\hat{\Psi}$	dimensionless stream function in the inner layer.

Subscripts

C	composite solution
H	constant wall heat flux case
T	constant wall temperature case
w	condition at the wall
∞	condition at infinity.

latter category has not received any attention so far even though it can be the dominant situation for high permeability porous media as well as near the leading edge for moderate to low permeability porous media. The objective of the present work is to study these two categories both analytically and numerically. The governing equations obtained by applying the method of matched asymptotic expansions for each category are solved both analytically using the modified Oseen method and numerically using the similarity transformation. As will be shown in the following sections, comparisons of the results for different categories reveal important characteristics related to the heat transfer and fluid flow.

2. FORMULATION OF THE PROBLEM

The steady two-dimensional natural convection about a semi-infinite vertical flat plate embedded in a fluid-saturated porous medium is considered. The schematics of the problem are shown in Fig. 1. It is assumed that the fluid and the solid matrix are in local thermodynamic equilibrium, and that the properties of the fluid and the porous matrix are constant and isotropic. Also inertia and thermal dispersion effects are neglected.

2.1. *Constant wall temperature case*

The governing equations for uniform porosity distribution, which are derived by using volume-averaged principles, are given as [1–9]

$$\frac{\partial u}{\partial x}+\frac{\partial v}{\partial y}=0 \tag{1}$$

$$Da_L\nabla^2\left(\frac{\partial u}{\partial y}-\frac{\partial v}{\partial x}\right)-\left(\frac{\partial u}{\partial y}-\frac{\partial v}{\partial x}\right)=-Ra_L\frac{\partial\theta}{\partial y} \tag{2}$$

$$u\frac{\partial\theta}{\partial x}+v\frac{\partial\theta}{\partial y}=\nabla^2\theta \tag{3}$$

where the pressure terms are eliminated and x, y, u, v, θ are nondimensionalized as

$$x^*=\frac{x}{L},\quad y^*=\frac{y}{L}$$

$$u^*=\frac{Lu}{\alpha_e},\quad v^*=\frac{Lv}{\alpha_e},\quad \theta=\frac{T-T_\infty}{T_w-T_\infty} \tag{4}$$

and * is dropped for convenience. In the above equations the Darcy number and the modified Rayleigh number are defined as

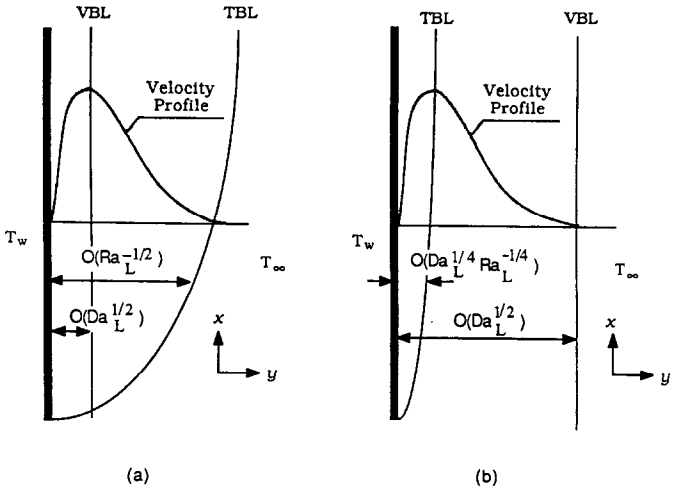

FIG. 1. Schematic of the physical model and coordinate system: (a) $\varepsilon_T \gg \varepsilon_V$; (b) $\varepsilon_T \ll \varepsilon_V$.

$$Da_L = \frac{1}{L^2}\frac{K}{\delta}, \quad Ra_L = \frac{Kg\beta L(T_w - T_\infty)}{\alpha_e \nu_f}. \tag{5}$$

Introducing the stream function

$$u = \frac{\partial \psi}{\partial y}, \quad v = -\frac{\partial \psi}{\partial x} \tag{6}$$

yields

$$Da_L(\psi_{xxxx} + 2\psi_{xxyy} + \psi_{yyyy}) - (\psi_{xx} + \psi_{yy}) = -Ra_L\,\theta_y \tag{7}$$

$$\psi_y\theta_x - \psi_x\theta_y = \theta_{xx} + \theta_{yy}. \tag{8}$$

The appropriate boundary conditions for this case are

$$\psi = \psi_y = \theta - 1 = 0 \quad \text{at } y = 0$$
$$\psi_y = \theta = 0 \quad \text{at } y \to \infty. \tag{9}$$

In the thermal boundary layer (TBL hereafter) where the heating effect of a vertical wall is felt, the heat conducted from the wall into the fluid is carried upwards by the convective movement of the fluid in the steady state. Hence the energy equation, equation (8), expressing a balance between convection and conduction gives

$$\psi \sim \frac{x}{\delta_T} \tag{10}$$

where δ_T denotes the thickness of the TBL. Turning our attention to the momentum balance in the same layer, we recognize the interaction between three forces, in equation (7). The first term denotes the boundary frictional force due to an impermeable boundary, the second term denotes the bulk frictional drag due to the porous medium, and the last term denotes the buoyancy force. Note that the buoyancy force is not negligible in the TBL since, without it, there would be no flow. Then

$$Da_L \frac{\psi}{\delta_T^4} \quad \text{or} \quad \frac{\psi}{\delta_T^2} \sim Ra_L \frac{1}{\delta_T}. \tag{11}$$

Combining equations (10) and (11) results in

$$Da_L\, Ra_L^{-1}\frac{x}{\delta_T^4} \quad \text{or} \quad Ra_L^{-1}\frac{x}{\delta_T^2} \sim 1. \tag{12}$$

From equation (12) it is clear that the TBL is ruled either by a 'boundary friction resistance ~ buoyancy force' balance or by a 'bulk frictional drag ~ buoyancy force' balance, depending on the magnitude of $Da_L^{1/2}/\delta_T$. From refs. [1, 8] it was shown that $Da_L^{1/2}$ is the order of magnitude of the viscous boundary layer (VBL hereafter) where the effect of boundary friction is felt. Hence to capture the physics of the problem attention will be given to two cases; one is when the thickness of the TBL is much larger than that of the VBL (Fig. 1(a)) and the other is for the reverse situation (Fig. 1(b)). The former will be denoted as Case TI and the latter as Case TII.

2.1.1. *Case* TI. $Ra_L^{-1/2} \gg Da_L^{1/2}$. Guided by the order of magnitude analysis it can be shown that in this case the free convective boundary layer consists of two regions where different phenomena are predominant. First there exists an outer region where the buoyancy term has to be of the same order of magnitude as the bulk friction term. In this region the fluid is driven upwards by buoyancy and restrained by bulk friction. This means that outside this layer, where the fluid is isothermal and the buoyancy effect is absent, the fluid is motionless. The velocity profile must then be as wide as the temperature profile, which is also the case for the regular fluid with a low Prandtl number. Second, there is an inner region where the boundary friction is of the same order of magnitude as the bulk friction as well as the buoyancy. Since the no-slip condition still applies at the wall, this layer can be considered as the region where the vertical velocity of the fluid varies from zero at the wall to its maximum value as shown in Fig. 1(a).

(1) The outer problem. From the order of magnitude analysis it can be shown that

$$\delta_T \sim x^{1/2} Ra_L^{-1/2}, \quad \psi \sim x^{1/2} Ra_L^{1/2}.$$

Hence introducing the outer variables as

$$Y = Ra_L^{1/2} y, \quad \Psi = Ra_L^{-1/2} \psi, \quad \Theta = \theta$$

where Y, Ψ and Θ are of the order of 1, transforms governing equations (7) and (8) into

$$\Psi_{YY} + \varepsilon_T^2 \Psi_{xx} = \Theta_Y + \Gamma_T^2(\Psi_{YYYY} + 2\varepsilon_T^2 \Psi_{xxYY} + \varepsilon_T^4 \Psi_{YYYY})$$

$$\Psi_Y \Theta_x - \Psi_x \Theta_Y = \Theta_{YY} + \varepsilon_T^2 \Theta_{xx}$$

subject to the boundary conditions

$$\Psi_Y = \Theta = 0 \quad \text{as } Y \to \infty.$$

Also Ψ and Θ must match with the inner solutions as $Y \to 0$. Here two parameters are defined as

$$\varepsilon_T = Ra_L^{-1/2}, \quad \Gamma_T = Da_L^{1/2} Ra_L^{1/2}. \tag{13}$$

Since the thickness of the VBL which is $O(Da_L^{1/2})$ is much smaller than that of the TBL which is $O(Ra_L^{-1/2})$, Γ_T, the ratio of these two, can be chosen as an expansion parameter. Expanding Ψ and Θ as

$$\Psi = \Psi_0 + \Gamma_T \Psi_1 + \Gamma_T^2 \Psi_2 + \cdots \tag{14a}$$

$$\Theta = \Theta_0 + \Gamma_T \Theta_1 + \Gamma_T^2 \Theta_2 + \cdots \tag{14b}$$

yields for the leading order

$$\Psi_{0YY} = \Theta_{0Y} \tag{15}$$

$$\Theta_{0YY} = \Psi_{0Y} \Theta_{0x} - \Psi_{0x} \Theta_{0Y}. \tag{16}$$

The boundary conditions are

$$\Psi_{0Y}(x, \infty) = \Theta_0(x, \infty) = 0. \tag{17a, b}$$

Also Ψ_0 and Θ_0 must match with the solutions for the inner layer as $Y \to 0$.

(2) The inner problem. From the order of magnitude analysis

$$\delta_V \sim Da_L^{1/2}, \quad \psi \sim Ra_L Da_L^{1/2}.$$

It is noticed that the velocity scale in this layer is dictated by the outer layer velocity scale in determining the order of magnitude for the stream function. Introducing the inner variables as

$$\hat{Y} = Da_L^{-1/2} y, \quad \hat{\Psi} = Ra_L^{-1} Da_L^{-1/2} \psi, \quad \hat{\Theta} = \theta$$

where $\hat{Y}$, $\hat{\Psi}$ and $\hat{\Theta}$ are of the order of 1 (note $\hat{Y} = Y/\Gamma_T$, $\hat{\Psi} = \Psi/\Gamma_T$), transforms governing equations (7) and (8) into

$$\hat{\Psi}_{\hat{Y}\hat{Y}} + \varepsilon_V^2 \hat{\Psi}_{xx} = \hat{\Theta}_{\hat{Y}} + \hat{\Psi}_{\hat{Y}\hat{Y}\hat{Y}\hat{Y}} + 2\varepsilon_V^2 \hat{\Psi}_{xx\hat{Y}\hat{Y}} + \varepsilon_V^4 \hat{\Psi}_{xxxx}$$

$$\hat{\Theta}_{YY} + \varepsilon_V^2 \hat{\Theta}_{xx} = \Gamma_T^2(\hat{\Psi}_{\hat{Y}} \hat{\Theta}_x - \hat{\Psi}_x \hat{\Theta}_{\hat{Y}})$$

where

$$\varepsilon_V = Da_L^{1/2} \tag{18}$$

subject to the boundary conditions

$$\hat{\Psi} = \hat{\Psi}_{\hat{Y}} = \hat{\Theta} - 1 = 0 \quad \text{as } \hat{Y} \to 0.$$

Also $\hat{\Psi}$ and $\hat{\Theta}$ must match with the outer solution as $\hat{Y} \to \infty$. Expanding $\hat{\Psi}$ and $\hat{\Theta}$ as

$$\hat{\Psi} = \hat{\Psi}_0 + \Gamma_T \hat{\Psi}_1 + \Gamma_T^2 \hat{\Psi}_2 + \cdots \tag{19a}$$

$$\hat{\Theta} = \hat{\Theta}_0 + \Gamma_T \hat{\Theta}_1 + \Gamma_T^2 \hat{\Theta}_2 + \cdots \tag{19b}$$

yields for the leading order

$$\hat{\Psi}_{0\hat{Y}\hat{Y}} = \hat{\Theta}_{0\hat{Y}} + \hat{\Psi}_{0\hat{Y}\hat{Y}\hat{Y}\hat{Y}} \tag{20}$$

$$\hat{\Theta}_{0\hat{Y}\hat{Y}} = 0. \tag{21}$$

The boundary conditions are

$$\hat{\Psi}_0(x, 0) = \hat{\Psi}_{0\hat{Y}}(x, 0) = \hat{\Theta}_0(x, 0) - 1 = 0. \tag{22a–c}$$

Also $\hat{\Psi}_0$ and $\hat{\Theta}_0$ must match with the solution for the outer layer as $\hat{Y} \to \infty$.

2.1.2. *Case* TII. $Ra_L^{-1/2} \ll Da_L^{1/2}$. Similar to Case TI, the free convection boundary layer for Case TII consists of two regions where different physical phenomena are predominant. First, there exists an inner region where tangible temperature differences with the ambient fluid exist. Only in this region are there buoyancy effects. The boundary friction is of the same order of magnitude as the buoyancy term. Second, there is an outer region where no buoyancy exists. The fluid in this region, however, is driven by viscous interaction with the inner layer as for the regular medium with a high Prandtl number. The bulk friction is of the same order of magnitude as the boundary friction.

(1) The inner problem. Based on the order of magnitude analysis

$$\delta_T \sim x^{1/4} Ra_L^{-1/4} Da_L^{1/4}, \quad \psi \sim x^{3/4} Ra_L^{1/4} Da_L^{-1/4}.$$

Hence introducing the inner variables as

$$\hat{Y} = Ra_L^{1/4} Da_L^{-1/4} y, \quad \hat{\Psi} = Ra_L^{-1/4} Da_L^{1/4} \psi, \quad \hat{\Theta} = \theta$$

where $\hat{Y}$, $\hat{\Psi}$ and $\hat{\Theta}$ are of the order of 1, transforms governing equations (7) and (8) as

$$\hat{\Theta}_{\hat{Y}} + \hat{\Psi}_{\hat{Y}\hat{Y}\hat{Y}\hat{Y}} + 2\eta_T^2 \hat{\Psi}_{xx\hat{Y}\hat{Y}} + \eta_T^4 \hat{\Psi}_{xxxx} = \Delta_T^2(\hat{\Psi}_{\hat{Y}\hat{Y}} + \eta_T^2 \hat{\Psi}_{xx})$$

$$\hat{\Psi}_{\hat{Y}} \hat{\Theta}_x - \hat{\Psi}_x \hat{\Theta}_{\hat{Y}} = \hat{\Theta}_{\hat{Y}\hat{Y}} + \eta_T^2 \hat{\Theta}_{xx}$$

subject to the boundary conditions

$$\hat{\Psi} = \hat{\Psi}_{\hat{Y}} = \hat{\Theta} - 1 = 0 \quad \text{at } \hat{Y} = 0.$$

Also $\hat{\Psi}$ and $\hat{\Theta}$ must match with the outer solution as $\hat{Y} \to \infty$. Here two parameters are defined as

$$\eta_T = Da_L^{1/4} Ra_L^{-1/4}, \quad \Delta_T = Da_L^{-1/4} Ra_L^{-1/4}. \tag{23}$$

Since the thickness of the TBL which is $O(Da_L^{1/4} Ra_L^{-1/4})$ is much smaller than that of the VBL which is $O(Da_L^{1/2})$, Δ_T, the ratio of these two can be chosen as an expansion parameter (note $\eta_T < \Delta_T$). Now expanding $\hat{\Psi}$ and $\hat{\Theta}$ as in equations (19) with a perturbation parameter Δ_T yields for the leading order

$$\hat{\Theta}_{0\hat{Y}} + \hat{\Psi}_{0\hat{Y}\hat{Y}\hat{Y}\hat{Y}} = 0 \tag{24}$$

$$\hat{\Theta}_{0\hat{Y}\hat{Y}} = \hat{\Psi}_{0\hat{Y}}\hat{\Theta}_{0x} - \hat{\Psi}_{0x}\hat{\Theta}_{0\hat{Y}}. \quad (25)$$

The boundary conditions are

$$\hat{\Psi}_0(x,0) = \hat{\Psi}_{0\hat{Y}}(x,0) = \hat{\Theta}_0(x,0) - 1 = 0. \quad (26a\text{–}c)$$

Also $\hat{\Psi}_0$ and $\hat{\Theta}_0$ must match with the solutions for the outer layer as $\hat{Y} \to \infty$.

(2) The outer problem. From the order of magnitude analysis

$$\delta_V \sim Da_L^{1/2}, \quad \psi \sim x^{1/2} Ra_L^{1/2}.$$

It is noticed that the velocity scale in this layer is dictated by the inner layer velocity scale in determining the order of magnitude for the stream function. Now introducing the outer variables as

$$Y = Da_L^{-1/2} y, \quad \Psi = Ra_L^{-1/2}\psi, \quad \Theta = \theta$$

where Y, Ψ and Θ are of the order of 1 (note $Y = \Delta_T \hat{Y}$, $\Psi = \Delta_T \hat{\Psi}$), transforms governing equations (7) and (8) into

$$\Psi_{YY} + \eta_V^2 \Psi_{xx} = \Psi_{YYYY} + 2\eta_V^2 \Psi_{xxYY} + \eta_V^4 \Psi_{xxxx}$$

$$\Theta = 0$$

subject to the boundary condition

$$\Psi_Y = 0 \quad \text{as } Y \to \infty.$$

Also Ψ must match with the inner solution as $Y \to 0$. Here

$$\eta_V = Da_L^{1/2}. \quad (27)$$

Expanding Ψ as in equation (14a) with a perturbation parameter η_V yields for the leading order

$$\Psi_{0YY} = \Psi_{0YYYY}. \quad (28)$$

The boundary conditions are

$$\Psi_{0Y}(x,\infty) = 0 \quad (29)$$

and Ψ_0 must match with the solution for the inner layer as $Y \to 0$.

2.2. *Constant wall heat flux*

Consider the case where a uniform heat flux is applied to the vertical flat plate. Then by introducing the same dimensionless quantities and the stream functions as in Section 2.1 except for

$$\theta = \frac{T - T_\infty}{qL/k_e}$$

it can be shown that governing equations (1)–(3) reduce to

$$Da_L(\psi_{xxxx} + 2\psi_{xxyy} + \psi_{yyyy}) - (\psi_{xx} + \psi_{yy}) = -Ra_L^* \theta_y \quad (30)$$

$$\psi_y\theta_x - \psi_x\theta_y = \theta_{xx} + \theta_{yy} \quad (31)$$

where Ra_L^* is defined as

$$Ra_L^* = \frac{Kg\beta L^2 q}{\alpha_e \nu_f k_e}. \quad (32)$$

The appropriate boundary conditions for this case are

$$\psi = \psi_y = \theta_y + 1 = 0 \quad \text{at } y = 0$$

$$\psi_y \to 0, \quad \theta \to 0 \quad \text{as } y \to \infty.$$

The order of magnitude analysis in this case is similar to that used in Section 2.1. So the final results are going to be presented without any details and be used for the perturbation analysis. Note that this case is also divided into two categories as shown in Fig. 1 depending on the magnitude of $Da_L^{1/2}\, Ra_L^{*1/3}$, which can be considered as the thickness ratio of the VBL to that of the TBL. Cases HI and HII will be used to distinguish one category from the other as in Section 2.1.

2.2.1. *Case* HI. $Ra_L^{*-1/2} \gg Da_L^{1/2}$.

(1) The outer problem. From the order of magnitude analysis

$$\delta_T \sim x^{1/3} Ra_L^{*-1/3}, \quad \psi \sim x^{2/3} Ra_L^{*1/3}, \quad \theta \sim x^{1/3} Ra_L^{*-1/3}.$$

Hence introducing the outer variables as

$$Y = Ra_L^{*1/3} y, \quad \Psi = Ra_L^{*-1/3}\psi, \quad \Theta = Ra_L^{*1/3}\theta$$

where Y, Ψ and Θ are of the order of 1, transforms governing equations (30) and (31) into

$$\Psi_{YY} + \varepsilon_T^{*2}\Psi_{xx} = \Theta_Y + \Gamma_H^2(\Psi_{YYYY} + 2\varepsilon_T^{*2}\Psi_{xxYY} + \varepsilon_T^{*4}\Psi_{xxxx})$$

$$\Psi_Y\Theta_x - \Psi_x\Theta_Y = \Theta_{YY} + \varepsilon_T^{*2}\Theta_{xx}$$

subject to the boundary conditions

$$\Psi_Y = \Theta = 0 \quad \text{as } Y \to \infty.$$

Also Ψ and Θ must match with the inner solutions as $Y \to 0$. Here two parameters are defined as

$$\varepsilon_T^* = Ra_L^{*-1/3}, \quad \Gamma_H = Da_L^{1/2}\, Ra_L^{*1/3}. \quad (33)$$

Expanding Ψ and Θ as in equations (14) with an expansion parameter Γ_H yields for the leading order

$$\Psi_{0YY} = \Theta_{0Y} \quad (34)$$

$$\Theta_{0YY} = \Psi_{0Y}\Theta_{0x} - \Psi_{0x}\Theta_{0Y}. \quad (35)$$

The boundary conditions are

$$\Psi_{0Y}(x,\infty) = \Theta_0(x,\infty) = 0. \quad (36a, b)$$

Also Ψ_0 and Θ_0 must match with the solutions for the inner layer as $Y \to 0$.

(2) The inner problem. From the order of magnitude analysis

$$\delta_V \sim Da_L^{1/2}, \quad \psi \sim x^{1/3} Da_L^{1/2} Ra_L^{*2/3}, \quad \theta \sim x^{1/3} Ra_L^{*-1/3}.$$

Hence introducing the inner variables as

$$\hat{Y} = Da_L^{-1/2} y, \quad \hat{\Psi} = Ra_L^{*-2/3} Da_L^{-1/2}\psi,$$

$$\hat{\Theta} = Ra_L^{*1/3}\,\theta$$

where $\hat{Y}$, $\hat{\Psi}$ and $\hat{\Theta}$ are of the order of 1 (note $\hat{Y} = Y/\Gamma_H$, $\hat{\Psi} = \Psi/\Gamma_H$), transforms governing equations (30) and (31) into

$$\hat{\Psi}_{\hat{Y}\hat{Y}} + \varepsilon_V^2 \hat{\Psi}_{XX} = \hat{\Theta}_{\hat{Y}} + \hat{\Psi}_{\hat{Y}\hat{Y}\hat{Y}\hat{Y}} + 2\varepsilon_V^2 \hat{\Psi}_{xx\hat{Y}\hat{Y}} + \varepsilon_V^4 \hat{\Psi}_{xxxx}$$

$$\hat{\Theta}_{\hat{Y}\hat{Y}} + \varepsilon_V^2 \hat{\Theta}_{xx} = \Gamma_H^2 (\hat{\Psi}_{\hat{Y}} \hat{\Theta}_x - \hat{\Psi}_x \hat{\Theta}_{\hat{Y}})$$

subject to the boundary conditions

$$\hat{\Psi} = \hat{\Psi}_{\hat{Y}} = 0, \quad \hat{\Theta}_{\hat{Y}} = -\Gamma_H \quad \text{at } \hat{Y} = 0.$$

Also $\hat{\Psi}$ and $\hat{\Theta}$ must match with the outer solution as $\hat{Y} \to \infty$. Expanding $\hat{\Psi}$ and $\hat{\Theta}$ as in equations (19) with a perturbation parameter Γ_H yields for the leading order

$$\hat{\Psi}_{0\hat{Y}\hat{Y}} = \hat{\Theta}_{0\hat{Y}} + \hat{\Psi}_{0\hat{Y}\hat{Y}\hat{Y}\hat{Y}} \tag{37}$$

$$\hat{\Theta}_{0\hat{Y}\hat{Y}} = 0. \tag{38}$$

The boundary conditions are

$$\hat{\Psi}_0(x,0) = \hat{\Psi}_{0\hat{Y}}(x,0) = \hat{\Theta}_{0\hat{Y}}(x,0) = 0. \tag{39a–c}$$

Also $\hat{\Psi}_0$ and $\hat{\Theta}_0$ must match with the solutions for the outer layer as $\hat{Y} \to \infty$. Even though the boundary conditions for the leading order inner problem do not seem to represent the constant wall heat flux condition, we can overcome this difficulty by imposing the constant heat flux condition at the wall on the outer solution since for the temperature the composite solution for the leading order is identical to the outer solution itself as will be shown later.

2.2.2. *Case* HII. $Ra_L^{*-1/3} \ll Da_L^{1/2}$.

(1) The inner problem. From the order of magnitude analysis

$$\delta_T \sim x^{1/5} Ra_L^{*-1/5} Da_L^{1/5}, \quad \psi \sim x^{4/5} Ra_L^{*1/5} Da_L^{-1/5},$$

$$\theta \sim x^{1/5} Ra_L^{*-1/5} Da_L^{1/5}.$$

Hence introducing the inner variables as

$$\hat{Y} = Ra_L^{*1/5} Da_L^{-1/5}\, y, \quad \hat{\Psi} = Ra_L^{*-1/5} Da_L^{1/5}\, \psi,$$

$$\hat{\Theta} = Ra_L^{*1/5} Da_L^{-1/5}\, \theta$$

where $\hat{Y}$, $\hat{\Psi}$ and $\hat{\Theta}$ are of the order of 1, transforms governing equations (30) and (31) into

$$\hat{\Theta}_{\hat{Y}} + \hat{\Psi}_{\hat{Y}\hat{Y}\hat{Y}\hat{Y}} + 2\eta_T^{*2} \hat{\Psi}_{xx\hat{Y}\hat{Y}} + \eta_T^{*4} \hat{\Psi}_{xxxx} = \Delta_H^2 (\hat{\Psi}_{\hat{Y}\hat{Y}} + \eta_T^{*2} \hat{\Psi}_{xx})$$

$$\hat{\Psi}_{\hat{Y}} \Theta_x - \hat{\Psi}_x \hat{\Theta}_{\hat{Y}} = \hat{\Theta}_{\hat{Y}\hat{Y}} + \eta_T^{*2} \hat{\Theta}_{xx}$$

subject to the boundary conditions

$$\hat{\Psi} = \hat{\Psi}_{\hat{Y}} = \hat{\Theta}_{\hat{Y}} + 1 = 0 \quad \text{at } \hat{Y} = 0.$$

Also $\hat{\Psi}$ and $\hat{\Theta}$ must match with the outer solution as $\hat{Y} \to \infty$. Here two parameters are defined as

$$\eta_T^* = Ra_L^{*-1/5} Da_L^{1/5}, \quad \Delta_H = Ra_L^{*-1/5} Da_L^{-3/10}. \tag{40}$$

Expanding $\hat{\Psi}$ and $\hat{\Theta}$ as in equations (19) with a perturbation parameter Δ_H yields for the leading order

$$\hat{\Theta}_{0\hat{Y}} + \hat{\Psi}_{0\hat{Y}\hat{Y}\hat{Y}\hat{Y}} = 0 \tag{41}$$

$$\hat{\Theta}_{0\hat{Y}\hat{Y}\hat{Y}} = \hat{\Psi}_{0\hat{Y}} \hat{\Theta}_{0x} - \hat{\Psi}_{0x} \hat{\Theta}_{0\hat{Y}}. \tag{42}$$

The boundary conditions are

$$\hat{\Psi}_0(x,0) = \hat{\Psi}_{0\hat{Y}}(x,0) = \hat{\Theta}_{0\hat{Y}}(x,0) + 1 = 0. \tag{43a–c}$$

Also $\hat{\Psi}_0$ and $\hat{\Theta}_0$ must match with the solutions for the outer layer as $\hat{Y} \to \infty$.

(2) The outer problem. From the order of magnitude analysis

$$\delta_V \sim Da_L^{1/2}, \quad \psi \sim x^{3/5} Ra_L^{*2/5} Da_L^{1/10}.$$

Hence introducing the outer variables as

$$Y = Da_L^{-1/2}\, y, \quad \Psi = Ra_L^{*-2/5} Da_L^{-1/10}\, \psi$$

where Y and Ψ are of the order of 1 (note $Y = \Delta_H \hat{Y}$, $\Psi = \Delta_H \hat{\Psi}$), transforms the governing equations into

$$\Psi_{YY} + \eta_V^2 \Psi_{xx} = \Psi_{YYYY} + 2\eta_V^2 \Psi_{xxYY} + \eta_V^4 \Psi_{xxxx}$$

$$\Theta = 0$$

subject to the boundary conditions

$$\Psi_Y = 0 \quad \text{as } Y \to \infty.$$

Also Ψ must match with the inner solution as $Y \to 0$. Expanding Ψ as in equation (14a) with a perturbation parameter η_V yields for the leading order

$$\Psi_{0YY} = \Psi_{0YYYY}. \tag{44}$$

The boundary condition is

$$\Psi_{0Y}(x,\infty) = 0. \tag{45}$$

Also Ψ_0 must match with the solution for the inner layer as $Y \to 0$.

3. ANALYSIS AND SOLUTIONS

The procedure of obtaining analytical solutions by using the modified Oseen method in this section is similar to that described by Gill [17] to solve the boundary layer equations for Newtonian fluid convection in an enclosure. More recently this method of solution was employed successfully by Weber [18], Bejan [19], and Tong and Subramanian [6] to deal with free convective heat transfer in porous enclosures. Of engineering importance is the fact that the overall heat transfer results produced by these analyses agree well with experimental and numerical heat transfer data as pointed out by Bejan [19]. To check the validity of using this method for the present problem, numerical solutions are also obtained based on the similarity transformation.

3.1. *Case* TI

For the outer layer equations (15)–(17) are solved using the modified Oseen method. Inserting equation (15) into equation (16) gives

$$\Psi_{0YYY} + \Psi_{0x} \Psi_{0YY} - \Theta_{0x} \Psi_{0Y} = 0. \tag{46}$$

This equation is linearized by regarding Ψ_{0x} and Θ_{0x} as unknown functions of x, $a(x)$ and $b(x)$, respec-

tively. Here $a(x)$ and $b(x)$ can be considered as line-averaged functions at fixed x across the thermal boundary layer region. This admits a solution of the following form for equation (46):

$$\Psi_{0Y} = C_1(x)\,e^{r_1 Y} + C_2(x)\,e^{r_2 Y}$$

where

$$r_{1,2} = \frac{-a \pm (a^2+4b)^{1/2}}{2}.$$

Function $b(x)$ represents the average vertical temperature gradient Θ_{0x} at fixed x inside the TBL. Therefore, we expect $b(x)$ to be positive since as the cold fluid rises it warms up gradually. Consequently, the two roots $r_1(x)$, $r_2(x)$ are of opposite sign regardless of the sign of $a(x)$. Boundary condition (17a) is satisfied only if the positive root is discarded. Thus the velocity solution is of the form

$$\Psi_{0Y} = A_1(x)\,e^{-Y/\alpha(x)} \tag{47}$$

where for reasons soon to be evident, we find it convenient to write $-1/\alpha$ in place of the negative root.

Integrating equation (15) and using equations (17b) and (47) gives

$$\Psi_{0Y} = \Theta_0 = A_1(x)\,e^{-Y/\alpha(x)}.$$

Also the integration of the above equation gives

$$\Psi_0 = -\alpha(x)A_1(x)\,e^{-Y/\alpha(x)} + A_2(x).$$

On the other hand, for the inner layer equations (20)–(22) are easily integrated to yield

$$\hat{\Theta}_0 = 1 + A_3(x)\hat{Y}$$

$$\hat{\Psi}_0 = A_4(x)(1-\hat{Y}-e^{-\hat{Y}}).$$

The exponentially growing term is already discarded, since, with it, the matching cannot be achieved. To determine A_1, A_2, A_3, and A_4, matching conditions are used. Matching the outer solutions with the inner solutions, after rewriting the outer and the inner solutions in terms of the inner and the outer variables respectively and expanding as $\Gamma_T \to 0$, gives

$$A_1(x) = 1, \quad A_2(x) = \alpha(x), \quad A_3(x) = 0,$$

$$A_4(x) = -1.$$

Hence

$$\Psi_0 = \alpha(x)[1-e^{-Y/\alpha(x)}], \quad \Theta_0 = e^{-Y/\alpha(x)} \tag{48}$$

$$\hat{\Psi}_0 = e^{-\hat{Y}} + \hat{Y} - 1, \quad \hat{\Theta}_0 = 1. \tag{49}$$

The only thing that is remaining to complete the solutions is to determine $\alpha(x)$. Inserting equations (48) into the integral form of energy equation (16) and solving for $\alpha(x)$ yields

$$\alpha(x) = 2x^{1/2}.$$

The integration constant is set to zero since $\Theta_0 = 0$ at $x = 0$. Therefore

$$\Psi_0 = 2x^{1/2}[1-e^{-Y/2x^{1/2}}], \quad \Theta_0 = e^{-Y/2x^{1/2}}. \tag{50}$$

Hsu and Cheng [8] presented the same analytical solution as equations (49) for the inner layer and the similarity solution for the outer layer. Note that $\eta_1 = Y/x^{1/2}$ in equations (50) is the similarity variable used in ref. [8]. Comparison between the approximate analytical solution and the similarity solution will be given in Section 4.

3.2. *Case* TII

For the inner layer both the numerical solution using the similarity transformation and the analytical solution using the modified Oseen method as for the outer layer of Case TI can be obtained. For the analytical solution combining equations (24) and (25) yields

$$\hat{\Psi}_{0\hat{Y}\hat{Y}\hat{Y}\hat{Y}} + \hat{\Psi}_{0x}\hat{\Psi}_{0\hat{Y}\hat{Y}\hat{Y}} + \hat{\Theta}_{0x}\hat{\Psi}_{0\hat{Y}} = 0.$$

Using the modified Oseen method, the solution is of the form

$$\hat{\Psi}_{0\hat{Y}} = \sum_{n=1}^{4} d_n(x)\,e^{-\lambda_n(x)\hat{Y}}$$

where λ_n are the roots of the characteristic equation

$$\lambda^4 - a\lambda^3 + b = 0.$$

As pointed out in Appendix A of ref. [6], two roots have positive real parts while the other two have negative real parts. Since only the roots with positive real parts will satisfy the matching condition as $\hat{Y} \to \infty$, the solution becomes after using equation (26b)

$$\hat{\Psi}_{0\hat{Y}} = B_1(x)(e^{-\lambda_1(x)\hat{Y}} - e^{-\lambda_2(x)\hat{Y}})$$

where $\lambda_1(x)$ and $\lambda_2(x)$ are the roots with positive real parts. Now assume $\lambda_1 \ll \lambda_2$. This assumption is made so that the inner velocity will approach a finite function of x rather than 0. This point can be confirmed using the similarity solution. Then the inner solution for the temperature can be approximated as

$$\hat{\Theta}_0 = B_1(x)\lambda_2^2\,e^{-\lambda_2\hat{Y}}. \tag{51}$$

Using equation (26c) gives $B_1(x) = 1/\lambda_2^2$. Then by letting $\beta(x) = 1/\lambda_2(x)$

$$\hat{\Psi}_{0\hat{Y}} = \beta^2(x)(e^{-\lambda_1(x)\hat{Y}} - e^{-\hat{Y}/\beta(x)}),$$

$$\hat{\Theta}_0 = e^{-\hat{Y}/\beta(x)}. \tag{52}$$

Matching equations (52) with the outer solution requires $\lambda_1 = \Delta_T$, and using the integral form of equation (25) gives $\beta(x) = (8x/3)^{1/4}$. Then for the inner layer

$$\hat{\Psi}_0 = \left(\frac{8}{3}x\right)^{1/2}\left[\frac{1}{\Delta_T}(1-e^{-\Delta_T\hat{Y}}) - \left(\frac{8}{3}x\right)^{1/4}(1-e^{-\hat{Y}/(8x/3)^{1/4}})\right],$$

$$\hat{\Theta}_0 = e^{-\hat{Y}/(8x/3)^{1/4}}. \tag{53}$$

For the outer layer equation (28) is easily integrated. Using equation (29) together with matching leads to

$$\Psi_0 = \left(\frac{8}{3}x\right)^{1/2}(1-e^{-Y}), \quad \Theta_0 = 0. \tag{54}$$

On the other hand, for the inner layer, the numerical solution can be obtained using the similarity transformation

$$\eta_2 = \frac{\hat{Y}}{x^{1/4}}, \quad \hat{\Psi}_0 = x^{3/4} f_0(\eta_2), \quad \hat{\Theta}_0 = g_0(\eta_2).$$

Then equations (24) and (25) become

$$g_0' + f_0^{iv} = 0 \tag{55}$$

$$g_0'' + \tfrac{3}{4} f_0 g_0' = 0 \tag{56}$$

where a prime denotes differentiation with respect to η_2. The appropriate B.C.s are

$$f_0(0) = f_0'(0) = g_0(0) - 1 = 0 \tag{57a–c}$$

$$f_0''(\infty) = f_0'''(\infty) = g_0(\infty) = 0. \tag{58a–c}$$

Three boundary conditions, equations (58), are obtained from the matching with the outer solutions. This system of ODE is to be solved numerically using the fourth-order Runge–Kutta method with shooting procedures. Comparison between this numerical solution and the approximate analytical solution will be made in Section 4.

3.3. *Case* HI

For the outer layer using the modified Oseen method as in Case TI the solutions for equations (34) and (35) satisfying equations (36) are of the form

$$\Psi_{0Y} = \Theta_0 = C_1(x)\, e^{-Y/\gamma(x)}.$$

On the other hand for the inner layer the integration of equations (37) and (38) along with equations (39) gives

$$\hat{\Psi}_0 = C_2(x)(e^{-\hat{Y}} + \hat{Y} - 1), \quad \hat{\Theta}_0 = C_3(x).$$

From matching we have

$$C_1(x) = C_2(x) = C_3(x).$$

Hence

$$\hat{\Psi}_0 = C_1(x)(e^{-\hat{Y}} + \hat{Y} - 1), \quad \hat{\Theta}_0 = C_1(x).$$

Now the condition of constant heat flux at the wall can be imposed on the outer solution since for the temperature the composite solution which is uniformly valid throughout the domain is equivalent to the outer solution. In other words imposing

$$\Theta_{0Y}(x, 0) = -1$$

gives $C_1(x) = \gamma(x)$. By doing this we can resolve such a problem that in equation (39c) the constant heat flux condition at the wall seems to play no role for the leading order solution.

The only unknown, $\gamma(x)$, can be determined using the integral form of the energy equation, equation (35), as in Case TI.

Then the outer solutions are

$$\Psi_0 = (2x)^{2/3}(1 - e^{-Y/(2x)^{1/3}}),$$

$$\Theta_0 = (2x)^{1/3} e^{-Y/(2x)^{1/3}} \tag{59}$$

and the inner solutions are

$$\hat{\Psi}_0 = (2x)^{1/3}(e^{-\hat{Y}} + \hat{Y} - 1), \quad \hat{\Theta}_0 = (2x)^{1/3}. \tag{60}$$

On the other hand, for the outer layer, we can get the numerical solution using the similarity transformation

$$\zeta_1 = \frac{Y}{x^{1/3}}, \quad \Psi_0 = x^{2/3} F_0(\zeta_1), \quad \Theta_0 = x^{1/3} G_0(\zeta_1).$$

Then equations (34) and (35) become

$$F_0''' = G_0' \tag{61}$$

$$G_0'' = \tfrac{1}{3} F_0' G_0 - \tfrac{2}{3} F_0 G_0' \tag{62}$$

where a prime denotes differentiation with respect to ζ_1. The boundary conditions are

$$F_0(0) = G_0'(0) + 1 = 0 \tag{63a, b}$$

$$F_0'(\infty) = G_0(\infty) = 0. \tag{64a, b}$$

Two boundary conditions, equations (63), are obtained from the matching with the inner solutions.

3.4. *Case* HII

Following the procedure similar to that for Case TII yields for the inner layer

$$\hat{\Psi}_0 = (2x)^{3/5}\left[\frac{1}{\Delta_H}(1 - e^{-\Delta_H \hat{Y}}) - (2x)^{1/5}(1 - e^{-\hat{Y}/(2x)^{1/5}})\right], \quad \hat{\Theta}_0 = (2x)^{1/5} e^{-\hat{Y}/(2x)^{1/5}} \tag{65}$$

and for the outer layer

$$\Psi_0 = (2x)^{3/5} e^{-Y}, \quad \Theta_0 = 0. \tag{66}$$

On the other hand, for the inner layer, we can get the numerical solution using the similarity transformation

$$\zeta_2 = \frac{\hat{Y}}{x^{1/5}}, \quad \tilde{\Psi}_0 = x^{4/5} \tilde{f}_0(\zeta_2), \quad \tilde{\Theta}_0 = x^{1/5} \tilde{g}_0(\zeta_2).$$

Then equations (41) and (42) become

$$\tilde{g}_0' + \tilde{f}_0^{iv} = 0 \tag{67}$$

$$\tilde{g}_0'' = \tfrac{1}{5} \tilde{f}_0' \tilde{g}_0 - \tfrac{4}{5} \tilde{f}_0 \tilde{g}_0'. \tag{68}$$

Here a prime denotes differentiation with respect to ζ_2. The appropriate B.C.s are

$$\tilde{f}_0(0) = \tilde{f}_0'(0) = \tilde{g}_0'(0) + 1 = 0 \tag{69a–c}$$

$$\tilde{f}_0''(0)(\infty) = \tilde{f}_0'''(\infty) = \tilde{g}_0(\infty) = 0. \tag{70a–c}$$

Three boundary conditions, equations (70), are obtained from the matching with the outer solutions.

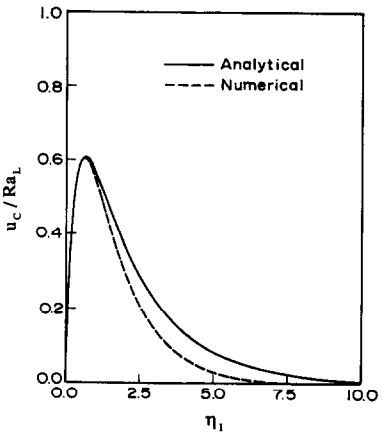

FIG. 2. Comparison between the analytical and numerical velocity distribution for Case TI, $\Gamma_T x^{-1/2} = 0.3$.

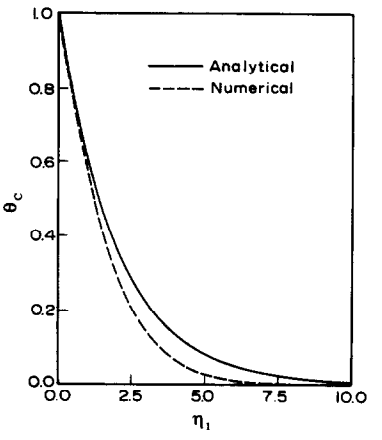

FIG. 3. Comparison between the analytical and numerical temperature distribution for Case TI.

4. RESULTS AND DISCUSSION

Composite solutions which are uniformly valid can be constructed by adding the inner and outer solutions and subtracting the common parts for stream function and temperature. From the results of the previous section, it is possible to get two different composite solutions depending on the method used. For example for the outer layer of Case TI, the modified Oseen method was used to get the analytical solution and the similarity transformation was used to obtain the numerical solution. To clarify this, the composite solutions for the former will be denoted as the analytical composite solutions and those for the latter will be denoted as the numerical composite solutions. In this section two different composite solutions for each of the streamwise velocity and the temperature will be given. Then the analytical composite solutions will be compared with the numerical composite solutions to check the validity of using the modified Oseen method for the present problem.

4.1. *Case* TI

From equations (49) and (50) the analytical composite solutions for the vertical velocity and the temperature can be written as

$$\frac{u_c}{Ra_L} = e^{-\eta_1/2} - e^{-\eta_1/(\Gamma_T x^{-1/2})} \tag{71a}$$

$$\theta_c = e^{-\eta_1/2} \tag{71b}$$

where $\eta_1 = Y/x^{1/2}$ is the similarity variable used in the numerical solution and $\Gamma_T x^{-1/2}$ is a parameter which can be considered as the local thickness ratio of the VBL to that of the TBL. Equation (71a) for $\Gamma_T x^{-1/2} = 0.3$ is presented in Fig. 2 along with the numerical solution in ref. [8]. Here the parameter $\Gamma_T x^{-1/2}$ represents the relative magnitude of the boundary effect; when $\Gamma_T x^{-1/2} = 0$ the solutions are identical to those based on Darcy's law where the viscous effects on the impermeable boundary are neglected. Also equation (71b) is presented in Fig. 3 along with the numerical solution in ref. [8]. As shown in Figs. 2 and 3 the agreement between analytical and numerical solutions is quite good, which confirms the use of the modified Oseen method to solve the natural convection problem about a vertical flat plate embedded in a porous medium.

4.2. *Case* TII

From equations (53) and (54) the analytical composite solutions for the vertical velocity and temperature can be written as

$$\frac{u_c}{Ra_L^{1/2}\, Da_L^{-1/2}} = \left(\frac{8}{3}x\right)^{1/2} [e^{-(\Delta_T x^{1/4})\eta_2} - e^{-\eta_2/(8/3)^{1/4}}] \tag{72a}$$

$$\theta_c = e^{-\eta_2/(8/3)^{1/4}} \tag{72b}$$

where $\eta_2 = \hat{Y}/x^{1/4}$ is the similarity variable used in the numerical solution and $\Delta_T x^{1/4}$ is a parameter which can be considered as the local thickness ratio of the TBL to that of the VBL. On the other hand, the numerical composite solutions for the vertical velocity and temperature can be written as

$$\frac{u_c}{Ra_L^{1/2}\, Da_L^{-1/2}} = x[f'_0(\infty)\{e^{-(\Delta_T x^{1/4})\eta_2} - 1\} - f'_0(\eta_2)] \tag{73a}$$

$$\theta_c = g_0(\eta_2). \tag{73b}$$

For comparison equations (72a) and (73a) are plotted in Fig. 4 for $\Delta_T x^{1/4} = 0.3$. Again the agreement between analytical and numerical solutions is good and as the local thick ratio $\Delta_T x^{1/4}$ increases the difference between two solutions for the vertical velocity is reduced. Hence for a fixed value of x, the agreement is improved as Δ_T is increased.

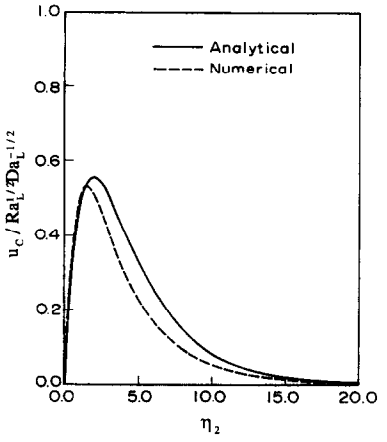

FIG. 4. Comparison between the analytical and numerical velocity distribution for Case TII, $\Delta_T x^{1/4} = 0.3$.

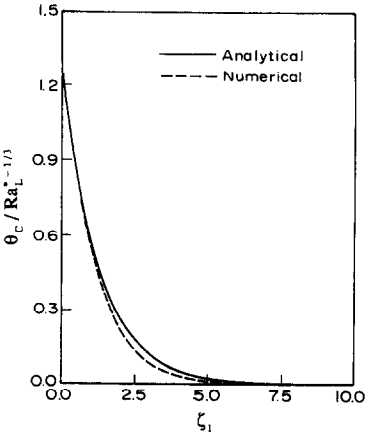

FIG. 6. Comparison between the analytical and numerical temperature distribution for Case HI.

4.3. *Case* HI

From equations (59) and (60) the analytical composite solutions for the vertical velocity and temperature can be written as

$$\frac{u_c}{Ra_L^{*2/3}} = (2x)^{1/3}[e^{-\zeta_1/2^{1/3}} - e^{-\zeta_1/(\Gamma_H x^{-1/3})}] \quad (74a)$$

$$\frac{\theta_c}{Ra_L^{*-1/3}} = (2x)^{1/3} e^{-\zeta_1/2^{1/3}} \quad (74b)$$

where $\zeta_1 = Y/x^{1/3}$ is the similarity variable used in the numerical solution and $\Gamma_H x^{-1/3}$ is a parameter that can be considered as the local thickness ratio of the VBL to that of the TBL. On the other hand the numerical composite solutions for the vertical velocity and temperature can be written as

$$\frac{u_c}{Ra_L^{*2/3}} = x^{1/3}[F_0'(\zeta_1) - F_0'(0) e^{-\zeta_1/(\Gamma_H x^{-1/3})}] \quad (75a)$$

$$\frac{\theta_c}{Ra_L^{*-1/3}} = x^{1/3} G_0(\zeta_1). \quad (75b)$$

For comparison equations (74a) and (75a) are presented in Fig. 5 for $\Gamma_H x^{-1/3} = 0.2$ and equations (74b) and (75b) are presented in Fig. 6. The agreement between analytical and numerical solutions is quite good as shown in these figures.

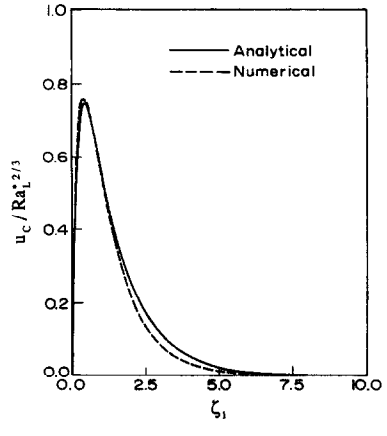

FIG. 5. Comparison between the analytical and numerical velocity distribution for Case HI, $\Gamma_H x^{-1/3} = 0.2$.

4.4. *Case* HII

From equations (65) and (66) the analytical composite solutions for the vertical velocity and temperature can be written as

$$\frac{u_c}{Ra_L^{*2/5} Da_L^{-2/5}} = (2x)^{3/5}[e^{-(\Delta_H x^{1/5})\zeta_2} - e^{-\zeta_2/2^{1/5}}] \quad (76a)$$

$$\frac{\theta_c}{Ra_L^{*-1/5} Da_L^{1/5}} = (2x)^{1/5} e^{-\zeta_2/2^{1/5}} \quad (76b)$$

where $\zeta_2 = \hat{Y}/x^{1/5}$ is the similarity variable used in the numerical solution and $\Delta_H x^{1/5}$ is a parameter which can be considered as the local thickness ratio of the TBL to that of the VBL. On the other hand, the numerical composite solutions for the vertical velocity and temperature can be written as

$$\frac{u_c}{Ra_L^{*2/5} Da_L^{-2/5}} = x^{3/5}[\tilde{f}_0'(\infty)\{e^{-(\Delta_H x^{1/5})\zeta_2} - 1\} + \tilde{f}_0'(\zeta_2)] \quad (77a)$$

$$\frac{\theta_c}{Ra_L^{*-1/5} Da_L^{1/5}} = x^{1/5} \tilde{g}_0(\zeta_2). \quad (77b)$$

For comparison equations (76a) and (77a) are plotted in Fig. 7 for $\Delta_H x^{1/5} = 0.2$.

From Figs. 2–7 it is noted that the no-slip boundary conditions have a drastic effect on the vertical velocity while these have little effect on the temperature field for the leading order as pointed out in ref. [8]. Also from Fig. 8 it can be concluded that for Cases TI and HI the maximum vertical velocity decreases from the slip velocity (using the Darcy model) as the local thickness ratio of the VBL to that of the TBL is increased from zero, and that the distance from the wall at which the vertical velocity has its maximum value increases with the value of this local thickness ratio. This local thickness ratio for these two cases

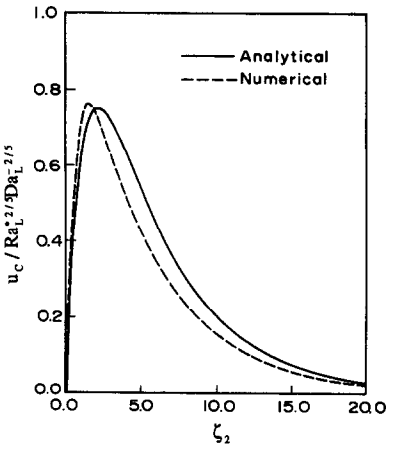

FIG. 7. Comparison between the analytical and numerical velocity distribution for Case HII, $\Delta_H x^{1/5} = 0.2$.

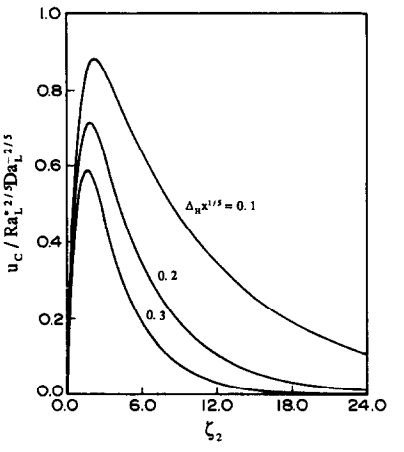

FIG. 9. Effects of the local thickness ratio on the vertical velocity for Case HII.

can be considered as the boundary parameter which was defined in refs. [8, 9], since for zero values of these parameters the results reduce to those based on the Darcy formulation and the viscous effect of the boundary increases with this parameter. On the other hand, for Cases TII and HII the maximum vertical velocity and the distance from the wall to which the fluid is affected by natural convection decrease as the local thickness ratio of the TBL to that of the VBL is increased, as shown in Fig. 9.

The most important result to be given is an expression for heat transfer. This can be presented conveniently by introducing the local Nusselt number

$$Nu_x = -\frac{x}{\theta_c(x,0)}\frac{\partial\theta_c(x,0)}{\partial y}.$$

The calculated values of the local Nusselt number for each case are presented in Table 1. Note that for Cases TI and HI, the Nusselt number depends only on the modified Rayleigh number. For Cases TII and HII, however, the Nusselt number depends on the Darcy number as well as the modified Rayleigh number. Also note that for Cases TI and HI the rate of heat transfer depends on the permeability of the porous medium, while for Cases TII and HII the rate of heat transfer is independent of the permeability of the porous medium, since the division of the modified Rayleigh number by the Darcy number results in the product of the Rayleigh number and the porosity. This result is very interesting and of physical importance. This finding can be inferred from equation (2) since the permeability of the porous medium does not appear explicitly if there is a balance between the boundary friction force and the buoyancy force. Hence it can be concluded that when the thickness of the VBL is much larger than that of the TBL, the heat transfer characteristics resemble those of the regular fluid with a large Prandtl number. This is because the Brinkman equation reduces to the Navier–Stokes equation as the permeability $K \to \infty$, while it reduces to the Darcy equation as $K \to 0$. Also, it is shown from the numerical solutions that the Nusselt numbers for Cases TI and HI are identical to those based on the Darcy flow model and the heat transfer rates for Cases TII and HII are very similar to those for a regular fluid of high Prandtl number. The only difference lies in that for Cases TII and HII the Rayleigh number is to be multiplied by the porosity in the expression for the Nusselt number. (See ref. [20] for numerical values for each case.) Finally, it is noticed that the analytical solution based on the modified Oseen method overpredicts the Nusselt number, which is inherent in this type of approach as pointed out in ref. [21].

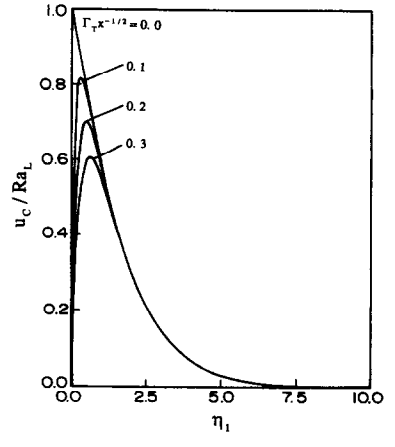

FIG. 8. Effects of the local thickness ratio on the vertical velocity for Case TI.

Table 1. The local Nusselt number

Case	Nu_x from analytical solution	Nu_x from numerical solution
TI	$0.5000 Ra_x^{1/2}$	$0.4438 Ra_x^{1/2}$
TII	$0.7825 Da_x^{-1/4} Ra_x^{1/4}$	$0.5027 Da_x^{-1/4} Ra_x^{1/4}$
HI	$0.7937 Ra_x^{*1/3}$	$0.7715 Ra_x^{*1/3}$
HII	$0.8706 Da_x^{-1/5} Ra_x^{*1/5}$	$0.6316 Da_x^{-1/5} Ra_x^{*1/5}$

5. CONCLUSION

The significance of the boundary effect on natural convection from a heated vertical plate embedded in a fluid-saturated porous medium has been thoroughly investigated. Consideration was given to flows which exhibit boundary layer characteristics for the constant wall temperature case and for the constant wall heat flux case. The method of matched asymptotic expansions was used to obtain the analytical solutions for both the velocity and the temperature fields. The full numerical solutions of all cases were also presented. For the case where the thickness of the thermal boundary layer is larger than that of the viscous boundary layer, the rate of heat transfer was found to depend only on the modified Rayleigh number. On the other hand for the case where the thickness of the viscous boundary layer is larger than that of the thermal boundary layer, the case which has never been considered before, the Nusselt number was found to depend on the product of the Rayleigh number and the porosity and to be independent of the permeability of the porous medium. Also, it was shown that for the latter case the heat transfer characteristics approach those of the regular fluid with a high Prandtl number.

REFERENCES

1. K. Vafai and C. L. Tien, Boundary and inertia effects on flow and heat transfer in porous media, *Int. J. Heat Mass Transfer* **24,** 195–203 (1981).
2. K. Vafai, Analysis of the channeling effect in variable porosity media, *J. Energy Resour. Technol.* **108,** 131–139 (1986).
3. K. Vafai and R. Thiyagaraja, Analysis of flow and heat transfer at the interface region of a porous medium, *Int. J. Heat Mass Transfer* **30,** 1391–1405 (1987).
4. M. Kaviany, Laminar flow through a porous channel bounded by isothermal parallel plates, *Int. J. Heat Mass Transfer* **28,** 851–858 (1985).
5. D. Poulikakos and K. Renken, Forced convection in a channel filled with porous medium, including the effects of flow inertia, variable porosity, and Brinkman friction, *J. Heat Transfer* **109,** 880–888 (1987).
6. T. W. Tong and E. Subramanian, A boundary layer analysis for natural convection in vertical porous enclosures—use of the Brinkman-extended Darcy model, *Int. J. Heat Mass Transfer* **28,** 563–571 (1985).
7. A. Bejan and D. Poulikakos, The non-Darcy regime for vertical boundary layer natural convection in a porous medium, *Int. J. Heat Mass Transfer* **27,** 717–722 (1984).
8. C. T. Hsu and P. Cheng, The Brinkman model for natural convection about a semi-infinite vertical flat plate in a porous medium, *Int. J. Heat Mass Transfer* **28,** 683–697 (1985).
9. J. T. Hong, C. L. Tien and M. Kaviany, Non-Darcian effects on vertical-plate natural convection in porous media with high porosities, *Int. J. Heat Mass Transfer* **28,** 2149–2157 (1985).
10. P. Cheng and W. J. Minkowycz, Free convection about a vertical flat plate embedded in a porous medium with application to a heat transfer from a dike, *J. Geophys. Res.* **82,** 2040–2044 (1977).
11. P. Cheng and C. T. Hsu, Higher-order approximations for Darcian free convective flow about a semi-infinite vertical flat plate, *J. Heat Transfer* **106,** 143–151 (1984).
12. Y. Joshi and B. Gebhart, Vertical natural convection flows in porous media: calculations of improved accuracy, *Int. J. Heat Mass transfer* **27,** 69–75 (1984).
13. O. A. Plumb and J. C. Huenefeld, Non-Darcy natural convection from heated surfaces in saturated porous media, *Int. J. Heat Mass Transfer* **24,** 765–768 (1981).
14. G. H. Evans and O. A. Plumb, Natural convection from a vertical isothermal surface embedded in a saturated porous medium, ASME Paper No. 78-HT-85 (1978).
15. M. Kaviany and M. Mittal, Natural convection heat transfer from a vertical plate to high permeability porous media: an experiment and an approximate solution, *Int. J. Heat Mass Transfer* **30,** 967–977 (1987).
16. J. T. Hong, Y. Yamada and C. L. Tien, Effects of non-Darcian and nonuniform porosity on vertical-plate natural convection in porous media, *J. Heat Transfer* **109,** 356–362 (1987).
17. A. E. Gill, The boundary-layer regime for convection in a rectangular cavity, *J. Fluid Mech.* **26,** 515–536 (1966).
18. J. E. Weber, The boundary-layer regime for convection in a vertical porous layer, *Int. J. Heat Mass Transfer* **18,** 569–573 (1975).
19. A. Bejan, On the boundary layer regime in a vertical enclosure filled with a porous medium, *Lett. Heat Mass Transfer* **6,** 93–102 (1979).
20. A. Bejan, *Convective Heat Transfer*, Chaps 4 and 10. Wiley, New York (1984).
21. G. Lauriat and V. Prasad, Natural convection in a vertical cavity: a numerical study for Brinkman-extended Darcy formulation, *J. Heat Transfer* **109,** 688–696 (1987).

ANALYSE DE LA CONVECTION NATURELLE CONTRE UNE PLAQUE VERTICALE NOYEE DANS UN MILIEU POREUX

Résumé—L'écoulement de convection naturelle et le transfert thermique autour d'une plaque plane verticale noyée dans un milieu poreux sont analysés dans deux cas généraux, celui de la température pariétale uniforme et celui du flux pariétal uniforme. Par une analyse d'ordre de grandeur, on montre qu'il y a deux paramètres adimensionnels qui sont reliés aux effets thermiques et de viscosité: $Ra_L^{-1/2}$ et $Da_L^{1/2}$ pour le cas de la température constante et $Ra_L^{*-1/3}$ et $Da_L^{1/2}$ pour le flux constant. Dans chaque cas, ces catégories sont physiquement reliées soit à $Da_L^{1/2} \ll Ra_L^{-1/2}$ ($Da_L^{1/2} \ll Ra_L^{*-1/3}$ pour le flux constant) soit à $Da_L^{1/2} \gg Ra_L^{-1/2}$ ($Da_L^{1/2} \gg Ra_L^{*-1/3}$ pour le flux constant). Ces équations sont résolues analytiquement par la méthode des développements asymptotiques avec la méthode modifiée d'Oseen. La solution numérique est obtenue aussi pour les équations, à partir de transformations affines. On trouve que le transfert thermique dépend du nombre de Rayleigh modifié pour $Da_L^{1/2} \ll Ra_L^{-1/2}$ (ou $Da_L^{1/2} \ll Ra_L^{*-1/3}$) tandis que le nombre de Nusselt dépend du produit du nombre de Rayleigh par la porosité pour $Da_L^{1/2} \gg Ra_L^{-1/2}$ (ou $Da_L^{1/2} \gg Ra_L^{*-1/3}$). Les caractéristiques de transfert thermique sont indépendantes de la perméabilité du milieu poreux et elles approchent celles du fluide régulier à grand nombre de Prandtl. Une description physique complète du problème est présentée à travers l'analyse.

UNTERSUCHUNG DER NATÜRLICHEN KONVEKTION AN EINER SENKRECHTEN PLATTE IN EINEM PORÖSEN MEDIUM

Zusammenfassung—Die Auftriebsströmung und der Wärmeübergang an einer senkrechten ebenen Platte in einem porösen Medium wurden für den Fall konstanter Wandtemperatur und für den Fall konstanten Wärmestroms detailliert untersucht. Durch eine Abschätzung der Größenordnung wird gezeigt, daß zwei dimensionslose Parameter die thermischen und viskosen Vorgänge im wesentlichen beschreiben. Es sind dies $Ra_L^{-1/2}$ und $Da_L^{1/2}$ im Fall konstanter Wandtemperatur und $Ra_L^{*-1/3}$ und $Da_L^{1/2}$ im Fall konstanten Wärmestroms. Für beide Fälle werden zwei wichtige Bereiche betrachtet. Bei konstanter Wandtemperatur sind die Bereiche entweder durch $Da_L^{1/2} \ll Ra_L^{-1/2}$ oder durch $Da_L^{1/2} \gg Ra_L^{-1/2}$ beschrieben. Bei konstantem Wärmestrom sind es entsprechend $Da_L^{1/2} \ll Ra_L^{*-1/3}$ und $Da_L^{1/2} \gg Ra_L^{*-1/3}$. Die Gleichungen wurden analytisch mit Hilfe der angepaßten asymptotischen Entwicklung gelöst unter Verwendung der modifizierten Oseen-Methode. Eine numerische Lösung auf der Grundlage der Ähnlichkeitstransformation wurde ebenfalls ermittelt. Das Wärmeübertragungsvermögen hängt von der modifizierten Rayleigh-Zahl ab, wenn $Da_L^{1/2} \ll Ra_L^{-1/2}$ (bzw. $Da_L^{1/2} \ll Ra_L^{*-1/3}$), während die Nusselt-Zahl vom Produkt aus Rayleigh-Zahl und Porosität abhängt, wenn $Da_L^{1/2} \gg Ra_L^{-1/2}$ (bzw. $Da_L^{1/2} \gg Ra_L^{*-1/3}$) ist. Die Wärmeübergangseigenschaften im letzteren Fall sind unabhängig von der Permeabilität des porösen Mediums und kommen denen eines normalen Fluids mit hoher Prandtl-Zahl nahe. Eine vollständige Beschreibung des Problems wird im Laufe der Untersuchung vorgestellt.

АНАЛИЗ ЕСТЕСТВЕННОЙ КОНВЕКЦИИ ОТ ПОМЕЩЕННОЙ В ПОРИСТУЮ СРЕДУ ВЕРТИКАЛЬНОЙ ПЛАСТИНЫ

Аннотация—Для двух общих случаев, а именно, постоянной температуры стенки и постоянной плотности теплового потока на стенке, детально анализируются свободноконвективное течение жидкости и теплоотдача от вертикальной плоской пластины, помещенной в пористую среду. Анализ порядка величин показал, что существуют два определяющих безразмерных параметра, связанных с тепловыми и вязкостными эффектами. Этими параметрами являются $Ra_L^{-1/2}$ и $Da_L^{1/2}$ для случая постоянной температуры и $Ra_L^{*-1/3}$ и $Da_L^{1/2}$ для постоянной плотности теплового потока на стенке. В каждом случае рассмотрены две важные ситуации. При постоянной температуре стенки это $Da_L^{1/2} \ll Ra_L^{-1/2}$($Da_L^{1/2} \ll Ra_L^{*-1/3}$) для постоянной плотности теплового потока на стенке) или $Da_L^{1/2} \gg Ra_L^{-1/2}$($Da_L^{1/2} \gg Ra_L^{*-1/3}$). Определяющие уравнения решаются аналитически методом сращиваемых асимптотических разложений совместно с модифицированным методом Озеена. Получено также численное решение определяющих уравнений, преобразованных с помощью метода подобия. Найдено, что коэффициент теплоотдачи зависит от модифицированного числа Рэлея для $Da_L^{1/2} \ll Ra_L^{-1/2}$ (или $Da_L^{1/2} \ll Ra_L^{*-1/3}$), а число Нуссельта зависит от произведения числа Рэлея и пористости среды для $Da_L^{1/2} \gg Ra_L^{-1/2}$ (или $Da_L^{1/2} \gg Ra_L^{*-1/3}$). Показано, что в последнем случае характеристики теплопереноса не зависят от проницаемости пористой среды и приближаются к характеристикам для обычной жидкости с высоким числом Прандтля. Дано полное физическое описание задачи.